

# Phosphate-binding Tag, a New Tool to Visualize Phosphorylated Proteins\*<sup>§</sup>

Eiji Kinoshita<sup>‡§¶</sup>, Emiko Kinoshita-Kikuta<sup>‡</sup>, Kei Takiyama<sup>‡</sup>, and Tohru Koike<sup>‡§||</sup>

**We introduce two methods for the visualization of phosphorylated proteins using alkoxide-bridged dinuclear metal (i.e. Zn<sup>2+</sup> or Mn<sup>2+</sup>) complexes as novel phosphate-binding tag (Phos-tag) molecules. Both Zn<sup>2+</sup>- and Mn<sup>2+</sup>-Phos-tag molecules preferentially capture phosphomonoester dianions bound to Ser, Thr, and Tyr residues. One method is based on an ECL system using biotin-pendant Zn<sup>2+</sup>-Phos-tag and horseradish peroxidase-conjugated streptavidin. We demonstrate the electroblotting analyses of protein phosphorylation status by the phosphate-selective ECL signals. Another method is based on the mobility shift of phosphorylated proteins in SDS-PAGE with polyacrylamide-bound Mn<sup>2+</sup>-Phos-tag. Phosphorylated proteins in the gel are visualized as slower migration bands compared with corresponding dephosphorylated proteins. We demonstrate the kinase and phosphatase assays by phosphate affinity electrophoresis (Mn<sup>2+</sup>-Phos-tag SDS-PAGE). *Molecular & Cellular Proteomics* 5: 749–757, 2006.**

Phosphorylation is a fundamental covalent post-translational modification that regulates the function, localization, and binding specificity of target proteins (1, 2). Organisms utilize this reversible reaction of proteins to control many cellular activities, including signal transduction, apoptosis, gene expression, cell cycle progression, cytoskeletal regulation, and energy metabolism. Abnormal protein phosphorylations are deeply related to carcinogenesis and neuropathogenesis. Methods for determining the phosphorylation status of proteins are thus very important with respect to the evaluation of diverse biological and pathological processes.

Recently we have reported that a dinuclear metal complex (i.e. 1,3-bis[bis(pyridin-2-ylmethyl)amino]propan-2-olato dizinc(II) complex) acts as a novel phosphate-binding tag (Phos-tag)<sup>1</sup> (commercially available at [www.phos-tag.com](http://www.phos-tag.com)) in

an aqueous solution at a neutral pH (e.g.  $K_d = 25$  nM for phenyl phosphate dianion) (4). The Phos-tag (see Fig. 1) has a vacancy on two metal ions that is suitable for the access of a phosphomonoester dianion as a bridging ligand. The resulting 1:1 phosphate-binding complex,  $\text{ROPO}_3^{2-}-(\text{Zn}^{2+}\text{-Phos-tag})^{3+}$ , has a total charge of +1. The anion selectivity indexes of the phenyl phosphate dianion against  $\text{SO}_4^{2-}$ ,  $\text{CH}_3\text{COO}^-$ ,  $\text{Cl}^-$ , and the bisphenyl phosphate monoanion at 25 °C are  $5.2 \times 10^3$ ,  $1.6 \times 10^4$ ,  $8.0 \times 10^5$ , and  $>2 \times 10^6$ , respectively. These findings have contributed to the development of procedures for MALDI-TOF-MS for the analysis of phosphorylated compounds (e.g. phosphopeptides and phospholipids) (5–7), IMAC for the separation of phosphopeptides and phosphorylated proteins (8), and surface plasmon resonance (SPR) analysis for reversible peptide phosphorylation (9). In this study, we demonstrated two novel applications of the Phos-tag molecules. One is the chemiluminescence detection of whole phosphorylated proteins on electroblotting membranes using biotinylated Zn<sup>2+</sup>-Phos-tag and HRP-SA. Another is simple SDS-PAGE for the separation of a phosphorylated protein and the corresponding nonphosphorylated one where polyacrylamide-bound Mn<sup>2+</sup>-Phos-tag was used as a phosphate-binding moiety.

## EXPERIMENTAL PROCEDURES

**Materials**—Acrylic acid, boric acid, bovine intestinal mucosa alkaline phosphatase (AP), bovine milk  $\alpha$ -casein, bovine milk  $\beta$ -casein, carbonic anhydrase, chicken egg ovalbumin, human serum albumin, NaCl, O-phosphorylserine, O-phosphoryltyrosine, and porcine pepsin were purchased from Sigma. 1-Ethyl-3-(3-dimethylaminopropyl)carbodiimide hydrochloride and 4-methoxyphenol were purchased from Tokyo Kasei Kogyo (Tokyo, Japan). Good's buffer, HEPES was purchased from Dojindo (Kumamoto, Japan). Thin-layer and silica gel column chromatographies were performed using a Merck silica gel TLC plate number 05554, silica gel 60 F<sub>254</sub> (Darmstadt, Germany), and Fuji Silysia Chemical NH-DM 1020 silica gel (Kasugai, Japan), respectively. Harmone (1-methyl-9H-pyrido[3,4-b]indole) and 2',4',6'-trihydroxyacetophenone were purchased from Aldrich. Bovine serum albumin was purchased from New England Biolabs (Beverly, MA).  $\beta$ -Galactosidase was purchased from Toyobo (Osaka, Japan). Ampholine (pH 3.5–10.0) for IEF, broad range protein molecular weight standards, ECL Plus Western blotting detection reagent, HRP-conjugated anti-mouse IgG antibody, HRP-conjugated anti-Tyr(P) monoclonal antibody (clone PY20), HRP-conjugated anti-rabbit IgG antibody, HRP-conjugated streptavidin, and PVDF membrane (Hybond P)

From the <sup>‡</sup>Department of Functional Molecular Science, Graduate School of Biomedical Sciences, and <sup>§</sup>Frontier Center for Microbiology, Hiroshima University, Kasumi 1-2-3, Hiroshima 734-8551, Japan Received, September 20, 2005, and in revised form, November 4, 2005

Published, MCP Papers in Press, December 11, 2005, DOI 10.1074/mcp.T500024-MCP200

<sup>1</sup> The abbreviations used are: Phos-tag, phosphate-binding tag; AP, alkaline phosphatase; EGF, epidermal growth factor; HRP, horseradish peroxidase; HRP-SA, horseradish peroxidase-conjugated streptavidin; TC-PTP, T-cell protein tyrosine phosphatase; SPR, surface plasmon resonance; CBB, Coomassie Brilliant Blue R-250; TE-

MED, *N,N,N',N'*-tetramethylethylenediamine; MAP, mitogen-activated protein; MBP, myelin basic protein; pMBP, phospho-MBP; HL, metal-free ligand; ADBI, assay dilution buffer I; 2-D, two-dimensional.

were purchased from Amersham Biosciences. Protein kinase A, recombinant human histone H1.2, and recombinant human T-cell protein tyrosine phosphatase (TC-PTP) were purchased from Calbiochem. A431 cell lysate, epidermal growth factor (EGF)-stimulated A431 cell lysate, and alkaline phosphatase-treated EGF-stimulated A431 cell lysate were purchased from Santa Cruz Biotechnology (Santa Cruz, CA). Rabbit anti-Ser(P) polyclonal antibody was purchased from Zymed Laboratories Inc.. Microcon YM30 and YM3 filter units were purchased from Millipore (Bedford, MA). Pro-Q Diamond phosphoprotein gel stain and SYPRO Ruby protein gel stain were purchased from Invitrogen. Acrylamide, 6-aminohexanoic acid, ammonium persulfate,  $\text{CH}_3\text{COONa}$ , Coomassie Brilliant Blue R-250 (CBB), glycerol, glycine, 2-mercaptoethanol, *N,N'*-methylenebisacrylamide, Nonidet P-40, disodium phenyl phosphate, SDS, TEMED, Tween 20, and tris(hydroxymethyl)aminomethane (Tris) were purchased from Nacalai Tesque (Kyoto, Japan). Anti-phospho-MAP kinase 1/2 (Erk1/2) antibody (clone 12D4), MAP kinase assay kit (containing myelin basic protein (MBP) and anti-pMBP monoclonal antibody), MEK1 assay kit (containing recombinant MEK1 and recombinant inactive MAP kinase 2/Erk2), recombinant Abl, recombinant Abltide-GST, and recombinant MAP kinase 2/Erk2 were purchased from Upstate Biotechnology (Lake Placid, NY). No. 3MM paper was purchased from Whatman. Acetone,  $\text{CHCl}_3$ ,  $\text{CH}_2\text{Cl}_2$ ,  $\text{CH}_3\text{CN}$ ,  $\text{CH}_3\text{COOH}$ , HCl,  $\text{H}_3\text{PO}_4$ , MeOH,  $\text{MnCl}_2$ , NaOH, and  $\text{Zn}(\text{NO}_3)_2 \cdot 6\text{H}_2\text{O}$  were purchased from Yoneyama Yakuhin Kogyo (Osaka, Japan). Bromphenol blue,  $\text{NaH}_2\text{PO}_4$ ,  $\text{NH}_3$ , and urea were purchased from Katayama Chemical (Osaka, Japan). All reagents and solvents used were of the highest commercial quality and used without further purification. All aqueous solutions were prepared using deionized and distilled water.

**Apparatus**—IR spectrum was recorded on a Horiba FT-710 infrared spectrometer with a KCl pellet (Real Crystal IR Card) at  $20 \pm 2^\circ\text{C}$ .  $^1\text{H}$  (500-MHz) and  $^{13}\text{C}$  (125-MHz) NMR spectra at  $25.0 \pm 0.1^\circ\text{C}$  were recorded on a JEOL LA500 spectrometer. Tetramethylsilane (in  $\text{CDCl}_3$ ) (Merck) was used as an internal reference for  $^1\text{H}$  and  $^{13}\text{C}$  NMR measurements. MALDI-TOF-MS spectra (positive reflector mode) were obtained on a Voyager RP-3 BioSpectrometry work station (PerSeptive Biosystems) equipped with a nitrogen laser (337 nm, 3-ns pulse). Time-to-mass conversion was achieved by external calibrations using peaks for  $\alpha$ -cyano-4-hydroxycinnamic acid ( $m/z$  190.05 for  $\text{M} + \text{H}^+$ ) and a peptide, Ac-Ile-Tyr-Gly-Glu-Phe- $\text{NH}_2$  ( $m/z$  691.31 for  $\text{M} + \text{Na}^+$ ). The pH measurement was conducted with a Horiba F-12 pH meter (Kyoto, Japan) and a combination pH electrode (Horiba-6378), which was calibrated using pH standard buffers (pH 4.01 and 6.86) at  $25^\circ\text{C}$ . Fluorescence gel images were acquired on an FLA 5000 laser scanner (Fujifilm, Tokyo, Japan). Pro-Q Diamond dye (10) was detected by 532-nm excitation with a 575-nm bandpass emission filter. SYPRO Ruby dye (11) was detected by 473-nm excitation with a 575-nm bandpass emission filter. A LAS 3000 image analyzer (Fujifilm) was used for the observation of chemiluminescence.

**Synthesis of Acrylamide-pendant Phos-tag Ligand**—Amino-pendant Phos-tag ligand (*N*-(5-(2-aminoethylcarbamoyl)pyridin-2-ylmethyl)-*N,N',N'*-tris(pyridin-2-yl-methyl)-1,3-diaminopropan-2-ol) was synthesized as described previously (8). A  $\text{CH}_2\text{Cl}_2$  solution (5 ml) of 1-ethyl-3-(3-dimethylaminopropyl)carbodiimide hydrochloride (92 mg, 0.48 mmol) was added dropwise to a solution of *N*-(5-(2-aminoethylcarbamoyl)pyridin-2-ylmethyl)-*N,N',N'*-tris(pyridin-2-yl-methyl)-1,3-diaminopropan-2-ol (0.21 g, 0.40 mmol), acrylic acid (35 mg, 0.48 mmol), and 4-methoxyphenol (0.30 mg) in 15 ml of  $\text{CH}_2\text{Cl}_2$  at  $0^\circ\text{C}$  for 5 min. The reaction mixture was stirred for 3 h at room temperature under a nitrogen atmosphere. After the solvent had been evaporated, the residue was dissolved in 100 ml of  $\text{CHCl}_3$ . The  $\text{CHCl}_3$  solution was washed with 0.5 M HEPES-NaOH buffer (pH 7.8, 50 ml  $\times$  5) and evaporated. The residue was purified by silica gel column chromatog-

raphy (eluent,  $\text{CH}_2\text{Cl}_2/\text{MeOH} = 50:0$  to  $50:1$ ) to obtain acrylamide-pendant Phos-tag ligand (*N*-(5-(2-acryloylaminoethylcarbamoyl)pyridin-2-ylmethyl)-*N,N',N'*-tris(pyridin-2-yl-methyl)-1,3-diaminopropan-2-ol) as a pale yellow oil (124 mg, 0.21 mmol, 53% yield). TLC (eluent,  $\text{CH}_3\text{CN}/\text{MeOH}/28\%$  aqueous  $\text{NH}_3 = 4:1:1$ )  $R_f = 0.70$ . IR ( $\text{cm}^{-1}$ ): 3263, 3061, 2928, 2828, 1652, 1594, 1569, 1539, 1478, 1436, 1408, 1365, 1316, 1248, 1150, 1122, 1094, 1048, 983, 806, 763, 733.  $^1\text{H}$  NMR ( $\text{CDCl}_3$ ):  $\delta$  2.56–2.69 (4H, m, NCCCHN), 3.57–3.66 (4H, m, CONCCH and CONCHC), 3.80–3.94 (9H, m, NCCHCN and PyCHN), 5.65 (1H, d,  $J = 10.3$  Hz, COC=CH), 6.11 (1H, dd,  $J = 17.0$  and  $10.3$  Hz, COCH=C), 6.29 (1H, d,  $J = 17.0$  Hz, COC=CH), 6.60 (1H, bs, NHCOC=C), 7.13 (3H, t,  $J = 6.2$  Hz, PyH), 7.34 (3H, d,  $J = 7.8$  Hz, PyH), 7.44 (2H, d,  $J = 8.0$  Hz, PyH), 7.59 (3H, td,  $J = 7.7$  and  $1.8$  Hz, PyH), 7.73 (1H, bs, PyCONH), 7.99 (1H, dd,  $J = 8.0$  and  $2.3$  Hz, PyH), 8.50 (3H, d,  $J = 4.3$  Hz, PyH), 8.90 (1H, d,  $J = 1.8$  Hz, PyH).  $^{13}\text{C}$  NMR ( $\text{CDCl}_3$ ):  $\delta$  39.7, 41.0, 58.9, 60.5, 60.8, 67.2, 122.0, 122.6, 123.0, 126.7, 128.0, 130.5, 135.4, 136.4, 147.7, 148.78, 148.83, 159.0, 159.2, 162.6, 166.4, 167.1. MALDI-TOF-MS: metal-free ligand (HL) in a 50% (v/v)  $\text{CH}_3\text{CN}$  solution containing 2',4',6'-trihydroxyacetophenone (5 mg/ml);  $m/z$  595.3 for  $\text{M} + \text{H}^+$ , 1:1 phosphate-bound dizinc(II) complex ( $\text{Zn}_2\text{L}^{3+}\text{-HOPO}_3^{2-}$ ) in a 50% (v/v)  $\text{CH}_3\text{CN}$  solution containing 2',4',6'-trihydroxyacetophenone (5 mg/ml), 1.0 mM  $\text{Zn}(\text{CH}_3\text{COO})_2$ , 0.50 mM HL, and 5.0 mM  $\text{NaH}_2\text{PO}_4\text{-NaOH}$  (pH 6.9);  $m/z$  817.1, 1:1 phenyl phosphate-bound dimanganese(II) complex ( $\text{Mn}_2\text{L}^{3+}\text{-PhOPO}_3^{2-}$ ) in a 50% (v/v) acetone solution containing Harmaline (5 mg/ml), 0.40 mM  $\text{MnCl}_2$ , 0.20 mM HL, 0.20 mM disodium phenyl phosphate, and 10 mM boric acid-NaOH (pH 9.0);  $m/z$  875.2.

**Preparation of a Complex of Biotin-pendant  $\text{Zn}^{2+}$ -Phos-tag and HRP-conjugated Streptavidin**—A MeOH solution of a biotin-pendant Phos-tag ligand (0.10 M) was diluted with an aqueous solution containing 10 mM Tris-HCl (pH 7.5), 0.10 M NaCl, and 0.1% (v/v) Tween 20 (TBS-T solution) by a factor of 10. The obtained solution of the 10 mM biotin-pendant Phos-tag ligand (solution L) was stored at room temperature. To prepare the 4:1 complex of biotin-pendant  $\text{Zn}^{2+}$ -Phos-tag and HRP-SA, solution L (10  $\mu\text{l}$ ), an aqueous solution of 10 mM  $\text{Zn}(\text{NO}_3)_2$  (20  $\mu\text{l}$ ), a commercially available solution of HRP-SA (1  $\mu\text{l}$ ), and TBS-T (469  $\mu\text{l}$ ) were mixed and allowed to stand for 30 min at room temperature. The mixed solution was put into a Microcon YM30 filter unit and centrifuged for 10 min at  $14,000 \times g$  to remove excess biotin-pendant  $\text{Zn}^{2+}$ -Phos-tag. The remaining solution ( $<10 \mu\text{l}$ ) in the reservoir was diluted with 30 ml of TBS-T solution and stored at  $4^\circ\text{C}$  ( $\text{Zn}^{2+}$ -Phos-tag-bound HRP-SA solution).

**SDS-PAGE**—Polyacrylamide gel electrophoresis was conducted according to Laemmli's method (12). Normal SDS-PAGE was usually performed at 35 mA/gel at room temperature in a 1-mm-thick, 9-cm-wide, and 9-cm-long gel on a PAGE apparatus (model AE6500; Atto, Tokyo, Japan). The gel consisted of 1.8 ml of a stacking gel (4.0% (w/v) polyacrylamide, 125 mM Tris-HCl (pH 6.8), and 0.1% (w/v) SDS) and 6.3 ml of a separating gel (7.5–12.5% (w/v) polyacrylamide, 375 mM Tris-HCl (pH 8.8), and 0.10% (w/v) SDS). For  $\text{Mn}^{2+}$ -Phos-tag SDS-PAGE, acrylamide-pendant Phos-tag ligand (50–150  $\mu\text{M}$ ) and 2 eq of  $\text{MnCl}_2$  were added to the separating gel before polymerization. An acrylamide stock solution was prepared as a mixture of a 29:1 ratio of acrylamide to *N,N'*-methylenebisacrylamide. The electrophoresis running buffer (pH 8.4) was 25 mM Tris and 192 mM glycine containing 0.1% (w/v) SDS. Sample proteins were resolved in an SDS-PAGE loading buffer (65 mM Tris-HCl (pH 6.8), 3.0% (w/v) SDS, 15% (v/v) 2-mercaptoethanol, 30% (v/v) glycerol, and 0.1% (w/v) bromphenol blue). The sample solutions were heated for 5 min at  $95^\circ\text{C}$  before gel loading.

**Pro-Q Diamond, SYPRO Ruby, and CBB Gel Staining**—After electrophoresis, gels were fixed in an aqueous solution containing 40% (v/v) MeOH and 10% (v/v)  $\text{CH}_3\text{COOH}$  for 30 min. To stain phosphorylated proteins with Pro-Q Diamond (10), the fixed gels were washed

in water for 30 min, incubated with Pro-Q Diamond phosphoprotein gel stain for 3 h, and then washed in 50 mM CH<sub>3</sub>COONa-CH<sub>3</sub>COOH (pH 4.0) buffer containing 20% (v/v) CH<sub>3</sub>CN for 3–12 h. For CBB staining, fixed gels were incubated with a CBB solution (0.1% (w/v) CBB, 10% (v/v) CH<sub>3</sub>COOH, and 40% (v/v) MeOH) for 1 h and then washed in an aqueous solution containing 25% (v/v) MeOH and 10% (v/v) CH<sub>3</sub>COOH until the background was clear. For SYPRO Ruby staining (11), fixed gels or Pro-Q Diamond-stained gels were incubated with SYPRO Ruby protein gel stain for 2 h and then washed in 25% (v/v) MeOH and 10% (v/v) CH<sub>3</sub>COOH for 2 h.

**Two-dimensional Polyacrylamide Gel Electrophoresis**—A431 cell lysate solved in a radioimmune precipitation assay buffer was de-salted using Microcon YM3 filter units and resolved in a sample buffer for IEF (9.5 M urea, 2% (w/v) Nonidet P-40, 2% (w/v) Ampholine, and 5% (v/v) 2-mercaptoethanol) to become 2.5 μg of protein/μl. An IEF disc gel (2-mm diameter and 12 cm long) consisted of 9.2 M urea, 4% (w/v) acrylamide, 0.2% (w/v) *N,N'*-methylenebisacrylamide, 0.1% (v/v) TEMED, 1.5% (w/v) Nonidet P-40, 2% (w/v) Ampholine, and 0.015% (w/v) ammonium persulfate. IEF was performed using Atto SJ-1060DCII. The electrode buffer of positive pole (11 mM H<sub>3</sub>PO<sub>4</sub>, 0.75 liter) was poured into the lower chamber, and the disc gels were set. Sample solutions (50 μg of protein/20 μl) were applied, 20 μl of a sample protection buffer (4.5 M urea and 1% (w/v) Ampholine) was put on the sample layer, and electrode buffer of negative pole (25 mM NaOH, 450 ml) was poured into the upper chamber. IEF was carried out at 400 V for 16 h at room temperature without cooling. After IEF electrophoresis, a disc gel was soaked twice for 15 min with a 0.25 M Tris-HCl (pH 6.8) buffer containing 2.5% (w/v) SDS, 5% (v/v) 2-mercaptoethanol, and 10% (w/v) glycerol. And then SDS-PAGE (12.5% (w/v) polyacrylamide) was performed at 50 mA/gel at room temperature using a 1-mm-thick, 13.5-cm-wide, and 13.5-cm-long gel (model AE-6200, Atto).

**Electroblotting**—The separated proteins in a polyacrylamide gel were electroblotted to PVDF membranes for 2 h using a semidry blotting system (Nippon Eido NB-1600, Tokyo, Japan) at 2 mA/cm<sup>2</sup> with three kinds of blotting solutions (solutions A, B, and C). After normal SDS-PAGE, the gel was soaked in solution B (25 mM Tris and 5% (v/v) MeOH) for 10 min. After Mn<sup>2+</sup>-Phos-tag SDS-PAGE, the gel was soaked in solution B containing 1.0 mM EDTA for 10 min and then soaked in solution B for 10 min. Three No. 3MM papers were soaked in solution A (25 mM Tris, 40 mM 6-aminohexanoic acid, and 5% (v/v) MeOH) and piled on the negative pole board. The gel, the PVDF membrane, and a piece of No. 3MM paper were soaked in solution B and piled up in order. Then two pieces of No. 3MM paper soaked in solution C (0.30 M Tris and 5% (v/v) MeOH) were piled up. Finally they were covered with the positive pole board, and electricity was supplied.

**Probing with Zn<sup>2+</sup>-Phos-tag-bound HRP-SA**—A protein-blotting PVDF membrane was soaked in a TBS-T solution at least for 1 h. The membrane was incubated with the Zn<sup>2+</sup>-Phos-tag-bound HRP-SA solution (1 ml/5 cm<sup>2</sup>) in a plastic bag for 30 min and washed twice with a TBS-T solution (10 ml/5 cm<sup>2</sup>) for 5 min each time at room temperature. The chemiluminescence was observed using an appropriate volume of ECL Plus solution.

**Probing with Antibody**—A blotting membrane was blocked by 1% (w/v) bovine serum albumin in TBS-T solution for 1 h. For detection of phosphorylated proteins on tyrosine residue, the membrane was probed with HRP-conjugated anti-Tyr(P) monoclonal antibody (clone PY20) (0.5 μg/ml in TBS-T, 1 ml/5 cm<sup>2</sup>) in a plastic bag for 1 h and washed twice with TBS-T solution (10 ml/5 cm<sup>2</sup>) each for 10 min, and then the chemiluminescence was observed. For detection of phosphorylated proteins on serine residue, the membrane was probed with rabbit anti-Ser(P) polyclonal antibody (1 μg/ml in TBS-T, 1 ml/5 cm<sup>2</sup>) in a plastic bag for 1 h, washed twice with TBS-T solution (10 ml/5 cm<sup>2</sup>) each for 10 min, probed with HRP-conjugated anti-rabbit

IgG antibody (0.1 μg/ml in TBS-T, 1 ml/5 cm<sup>2</sup>) in a plastic bag for 1 h, and washed twice with TBS-T solution (10 ml/5 cm<sup>2</sup>) each for 10 min, and then the chemiluminescence was observed. For detection of phosphorylated MBP on threonine residue, the membrane was probed with anti-pMBP monoclonal antibody (clone P12) (0.5 μg/ml in TBS-T solution, 1 ml/5 cm<sup>2</sup>) in a plastic bag for 1 h, washed twice with TBS-T solution (10 ml/5 cm<sup>2</sup>) each for 10 min, probed with HRP-conjugated anti-mouse IgG antibody (0.1 μg/ml in TBS-T, 1 ml/5 cm<sup>2</sup>) in a plastic bag for 1 h, and washed twice with TBS-T solution (10 ml/5 cm<sup>2</sup>) each for 10 min, and then the chemiluminescence was observed. For phosphorylated MAP kinase 1/2 (Erk1/2) detection, the membrane was probed with anti-phospho-MAP kinase 1/2 antibody (clone 12D4) (0.1 μg/ml in TBS-T solution, 1 ml/5 cm<sup>2</sup>) in a plastic bag for 1 h, washed twice with TBS-T solution (10 ml/5 cm<sup>2</sup>) each for 10 min, probed with HRP-conjugated anti-mouse IgG antibody (0.1 μg/ml in TBS-T, 1 ml/5 cm<sup>2</sup>) in a plastic bag for 1 h, and washed twice with TBS-T solution (10 ml/5 cm<sup>2</sup>) each for 10 min, and then the chemiluminescence was observed.

**Reprobing of the Blotting Membranes**—For elimination of biotin-pendant Zn<sup>2+</sup>-Phos-tag and HRP-SA or antibodies from the blotting membrane after ECL analysis, the membranes were incubated with a stripping buffer (25 ml/5 cm<sup>2</sup>) consisting of 62.5 mM Tris-HCl (pH 6.8), 2% (w/v) SDS, and 0.10 M 2-mercaptoethanol for 20 min at 50 °C and washed three times with TBS-T solution (25 ml/5 cm<sup>2</sup>) each for 1 h at room temperature, and remaining proteins on the membrane were probed with the other antibody.

**Kinase Assays**—Phosphorylations of Abltide-GST catalyzed with Abl, MBP catalyzed with MAP kinase, and unactive MAP kinase 2/Erk2 catalyzed with MEK1 were performed using assay dilution buffer I (ADBI), magnesium/ATP mixture substrate solutions, and enzyme solutions obtained from Upstate Biotechnology without any dilutions. The component of each solution was as follows. ADBI consists of 20 mM MOPS (pH 7.2), 25 mM β-glycerol phosphate, 5.0 mM EGTA, 1.0 mM sodium orthovanadate, and 1.0 mM dithiothreitol. Magnesium/ATP mixture consists of 75 mM MgCl<sub>2</sub> and 0.50 mM ATP in ADBI. Recombinant Abltide-GST (0.5 mg) was dissolved in 0.50 ml of 50 mM Tris-HCl (pH 8.0), 0.15 M NaCl, 20 mM glutathione, and 20% glycerol. MBP (2 mg) was dissolved in 1.0 ml of ADBI. Recombinant unactive MAP kinase 2/Erk2 (50 μg) was dissolved in 0.20 ml of 50 mM Tris-HCl (pH 7.5), 0.15 M NaCl, 0.10 mM EGTA, 0.03% Brij 35, 0.1% 2-mercaptoethanol, 1 mM benzamidine, 0.10 mM PMSF, and 50% glycerol. Recombinant Abl (5 μg) was dissolved in 50 μl of 50 mM Tris-HCl (pH 7.5), 0.27 M sucrose, 0.15 M NaCl, 1.0 mM benzamidine, 0.20 mM PMSF, 0.10 mM EGTA, 0.1% 2-mercaptoethanol, and 0.03% Brij 35. Recombinant MAP kinase 2/Erk2 (5 μg) was dissolved in 50 μl of 50 mM Tris-HCl (pH 7.5), 0.15 M NaCl, 0.10 mM EGTA, 0.03% Brij 35, 50% glycerol, 1.0 mM benzamidine, 0.20 mM PMSF, and 0.1% 2-mercaptoethanol. Recombinant MEK1 (5 μg) was dissolved in 50 μl of 50 mM Tris-HCl (pH 7.5), 0.10 mM EGTA, 0.15 M NaCl, 0.1% 2-mercaptoethanol, 0.03% Brij 35, 1.0 mM benzamidine, 0.20 mM PMSF, and 5% glycerol. Time-dependent phosphorylations of substrates were performed as follows. In the case of phosphorylation of Abltide-GST, 0.14 ml of ADBI, 39 μl of magnesium/ATP mixture, 20 μl of Abltide-GST (20 μg), and 1.0 μl of recombinant Abl (0.1 μg) were incubated at 30 °C. In the case of MBP, 29 μl of ADBI, 10 μl of magnesium/ATP mixture, 10 μl of MBP (20 μg), and 1.0 μl of recombinant MAP kinase 2/Erk2 (0.1 μg) were incubated at 30 °C. In recombinant unactive MAP kinase 2/Erk2, 148 μl of ADBI, 100 μl of magnesium/ATP mixture, 40 μl of recombinant unactive MAP kinase 2/Erk2 (10 μg), and 2 μl of recombinant MEK1 (0.2 μg) were incubated at 30 °C. Time-dependent phosphorylation of recombinant human histone H1.2 catalyzed with protein kinase A was performed in 50 μl of 50 mM Tris-HCl (pH 7.5), 10 mM MgCl<sub>2</sub>, 0.20 mM ATP, 40 μg of histone H1.2, and 2,500 units of protein kinase A at 37 °C. The

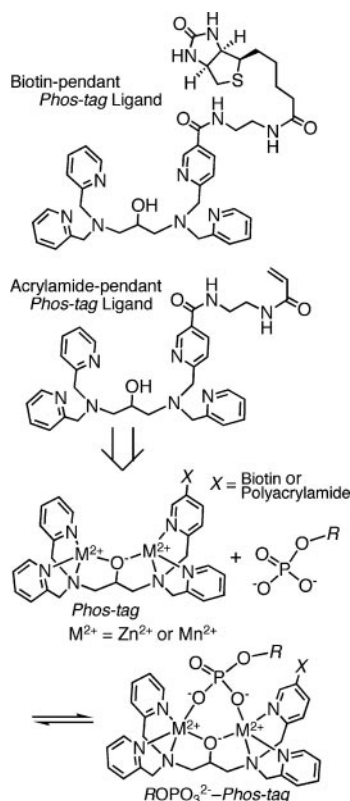


FIG. 1. Structures of biotin-pendant and acrylamide-pendant Phos-tag ligands and scheme of the reversible capturing of a phosphomonoester dianion (ROPO<sub>3</sub><sup>2-</sup>) by Zn<sup>2+</sup>-Phos-tag and Mn<sup>2+</sup>-Phos-tag.

phosphorylation reactions were stopped by addition of a half-volume of 3× SDS-PAGE loading buffer. Zero time samples were prepared using the same components without the enzymes.

**Phosphatase Assays**—Dephosphorylated samples of phosphoproteins were prepared using a 50 mM Tris-HCl buffer (pH 9.0, 0.20 ml) containing 1.0 mM MgCl<sub>2</sub>, 50 μg of protein, and 3.3 units of alkaline phosphatase (incubation at 37 °C for 12 h and then mixing with 0.10 ml of 3× SDS-PAGE loading buffer). Time-dependent dephosphorylation of bovine milk β-casein was performed in a 50 mM Tris-HCl buffer (pH 9.0, 0.14 ml) containing 1.0 mM MgCl<sub>2</sub>, 0.7 mg of protein, and 165 microunits of alkaline phosphatase at 37 °C. Phosphorylated Abltide-GST was prepared as mentioned above, and the solution of the kinase reaction was used in the tyrosine phosphatase assay. Time-dependent dephosphorylation of phosphorylated Abltide-GST was performed in 50 mM Tris-HCl buffer (pH 7.0, 0.20 ml) containing 20 μl of phosphorylated Abltide-GST (2 μg) solution, and 0.3 unit of TC-PTP at 30 °C. The dephosphorylation reactions were stopped by addition of a half-volume of 3× SDS-PAGE loading buffer. Zero time samples were prepared using the same components without the enzymes.

## RESULTS

**Specific Visualization of Phosphorylated Proteins on a Blotting Membrane**—To visualize phosphorylated proteins, we determined the potency of biotin-pendant Zn<sup>2+</sup>-Phos-tag (9) (see Fig. 1) as a phosphate-binding biotin derivative for Western blotting analysis. As the first example, phosphorylated proteins (*i.e.* α-casein, β-casein, ovalbumin, and pepsin) spot-

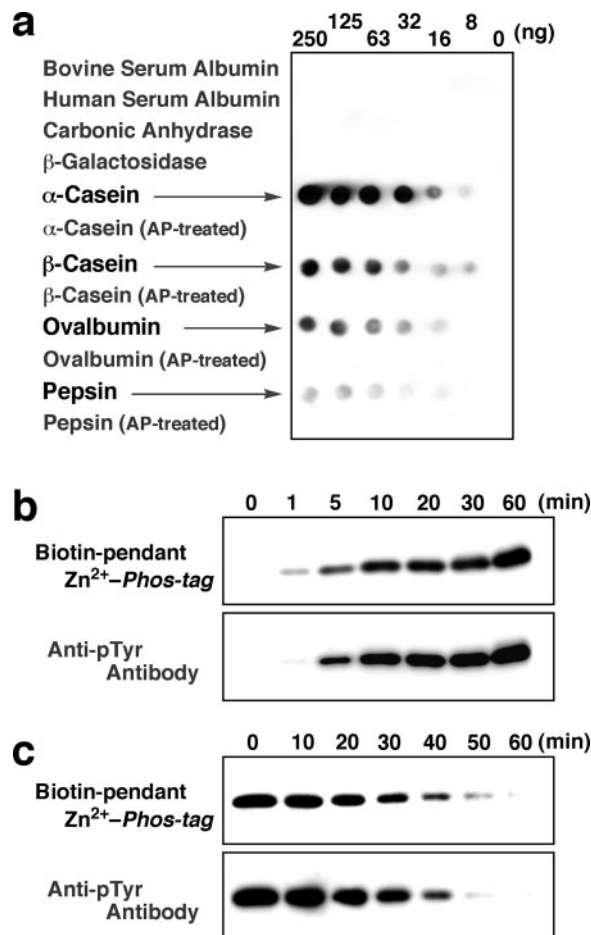


FIG. 2. Chemiluminescence detection of phosphorylated proteins on PVDF membranes using biotin-pendant Zn<sup>2+</sup>-Phos-tag and HRP-SA. *a*, dot-blotting analysis of four nonphosphorylated proteins (bovine serum albumin, human serum albumin, carbonic anhydrase, and β-galactosidase), four phosphorylated proteins (α-casein, β-casein, ovalbumin, and pepsin), and the corresponding dephosphorylated proteins (AP-treated). *b*, electroblotting analysis of the phosphorylation of Abltide-GST (0.13 μg of protein/lane) incubated with a tyrosine kinase, Abl. *c*, electroblotting analysis of the dephosphorylation of phosphorylated Abltide-GST (50 ng of proteins/lane) incubated with a tyrosine phosphatase, TC-PTP. After elimination of biotin-pendant Zn<sup>2+</sup>-Phos-tag and HRP-SA from the membranes (*b* and *c*), the remaining phosphorylated Abltide-GST was probed using the HRP-anti-Tyr(P) antibody. The incubation time is shown above each lane. *pTyr*, phosphotyrosine.

ted on a PVDF membrane were specifically detected at nanogram levels using an ECL system and a 4:1 complex of biotin-pendant Zn<sup>2+</sup>-Phos-tag and HRP-SA without a blocking treatment of the membrane. A typical ECL image by dot-blotting analysis is shown in Fig. 2a. No ECL signal was detected on the spots of the corresponding dephosphorylated proteins and the nonphosphorylated proteins (*i.e.* bovine serum albumin, human serum albumin, carbonic anhydrase, and β-galactosidase). In the absence of the zinc(II) ions (*i.e.* using a 4:1 complex of biotin-pendant Phos-tag ligand and HRP-SA in the presence of 1 mM EDTA), no ECL signals were

detected on the spots of phosphorylated proteins (data not shown). Thus, the phosphate-selective ECL signals were produced by the complex of biotin-pendant  $Zn^{2+}$ -Phos-tag and HRP-SA via the interaction between the zinc(II) ions and the phosphomonoester dianion.

Next we applied the complex of biotin-pendant  $Zn^{2+}$ -Phos-tag and HRP-SA to an electroblotting analysis after SDS-PAGE. This application did not require a blocking treatment of a PVDF membrane. The phosphorylation of Abltide-GST incubated with a tyrosine kinase, Abl, and the dephosphorylation of phosphorylated Abltide-GST incubated with a tyrosine phosphatase, TC-PTP, were visualized on PVDF membranes. The Abltide-GST is a recombinant fusion protein of an Abl substrate peptide (Abltide, Glu-Ala-Ile-Tyr-Ala-Ala-Pro-Phe-Ala-Lys-Lys-Lys) tagged by a GST. The Tyr<sup>4</sup> residue (italicized) of the Abltide section is selectively phosphorylated by Abl. The time courses of the phosphorylation and dephosphorylation are shown in Fig. 2, *b* and *c*, respectively. Both ECL detections were successively confirmed by a conventional procedure, immunoprobings with the anti-Tyr(P) monoclonal antibody (clone PY20) of the same blots. We also demonstrated similar electroblotting analyses of the phosphorylation of MAP kinase (phosphorylated on the Thr<sup>183</sup> and Tyr<sup>185</sup> residues) incubated with MEK1 (a Tyr and Ser/Thr dual kinase) and the phosphorylation of histone H1.2 incubated with protein kinase A (a Ser/Thr kinase) (Supplemental Fig. 1). These results indicate that biotin-pendant  $Zn^{2+}$ -Phos-tag captures various phosphorylated proteins bound on a PVDF membrane.

**Visualization of the Protein Phosphorylation Status of A431 Cells**—We extended the phosphate-specific detection to the analysis of the phosphorylation status of A431 human epidermoid carcinoma cells before and after EGF stimulation. The EGF-dependent protein phosphorylations in the A431 cell have been well established (13–23); therefore, we selected the cell as the first biological sample. For one-dimensional SDS-PAGE (Fig. 3, *a–g*), the molecular weight standards (*lane M*), the lysate of the cells before (*lane 1*) or after EGF stimulation (*lane 2*), and the AP-treated lysate of the cells after EGF stimulation (*lane 3*) were sequentially applied. Fluorescent gel staining with SYPRO Ruby (Fig. 3*a*) showed that the total proteins of the lysate applied in each lane were almost equal. Pro-Q Diamond gel staining (Fig. 3*b*) showed the increase of phosphorylated proteins by EGF stimulation and the decrease of dephosphorylated proteins by AP treatment. Electroblotting analysis using the 4:1 complex of biotin-pendant  $Zn^{2+}$ -Phos-tag and HRP-SA (Fig. 3*c*) demonstrated that the ECL signals can represent the phosphorylation status of A431 cells more clearly than the fluorescent gel staining (Fig. 3*b*). The ECL signals increased by EGF stimulation (*lane 2*) were greatly diminished by AP treatment of the lysate (*lane 3*), indicating that the visualized proteins as ECL signals are phosphorylated proteins. The electroblotting analysis also detected a phosphorylated protein, ovalbumin (45 kDa), in the molecular weight standards (Fig. 3*b*, *lane M*). In electro-

blotting analysis using only HRP-SA, some proteins (e.g. a biotinylated endogenous protein) in the lysate were detected as ECL signals (Fig. 3*d*). Electroblotting analysis using the 4:1 complex of the biotin-pendant Phos-tag ligand and HRP-SA in the presence of 1 mM EDTA (Fig. 3*e*) showed, however, that the ECL signals (Fig. 3, *c* and *d*) disappeared completely. These facts suggested that the zinc(II) complexation and the binding of the biotin-pendant to HRP-SA are essential for phosphate-specific detection. The proteins of the cell lysate were also analyzed by immunoblotting using the anti-Tyr(P) antibody (Fig. 3*f*) and the anti-Ser(P) polyclonal antibody (Fig. 3*g*). With regard to monitoring the change in the phosphorylation status, the data of the blotting analysis using biotin-pendant  $Zn^{2+}$ -Phos-tag were compatible with these results obtained with conventional methods using antibodies. In all electroblotting analyses, a nonspecific ECL signal of a marker protein, lysozyme (14 kDa in *lane M*), was observed using the ECL system (Fig. 3, *c–g*).

Next we determined the protein phosphorylation status of the EGF-stimulated cells by two-dimensional (2-D) IEF/SDS-PAGE followed by an electroblotting analysis as shown in Fig. 3*h*. The ECL signal intensity and number of spots on the membrane remarkably increased in comparison with those before EGF stimulation (see Supplemental Fig. 2). After the ECL detection with biotin-pendant  $Zn^{2+}$ -Phos-tag, the same membrane was sequentially reprobed with the anti-Tyr(P) antibody and the anti-Ser(P) antibody. Superimposed images of the area surrounded with a *dotted square* in Fig. 3*h* were obtained by using biotin-pendant  $Zn^{2+}$ -Phos-tag (*green*) and the anti-Tyr(P) antibody (*magenta*) (Fig. 3*i*) and biotin-pendant  $Zn^{2+}$ -Phos-tag (*green*) and the anti-Ser(P) antibody (*magenta*) (Fig. 3*j*). Some proteins detected by both biotin-pendant  $Zn^{2+}$ -Phos-tag and the antibodies appear as *white spots* in the superimposed images.

**Separation of Phosphorylated Proteins in a Polyacrylamide Gel**—We synthesized an acrylamide-pendant Phos-tag ligand (see Fig. 1 and “Experimental Procedures”) as a novel additive (i.e. a copolymer) of the separating gel for the visualization of phosphorylated proteins by SDS-PAGE. The principle of this detection is the mobility shift of phosphorylated proteins due to reversible phosphate trapping by Phos-tag molecules immobilized in the gel. First we applied a polyacrylamide-bound  $Zn^{2+}$ -Phos-tag to SDS-PAGE according to the widely accepted Laemmli method (12). However, the expected phosphate-selective mobility shift was not observed under such general SDS-PAGE conditions (data not shown). Presumably the alkaline condition (more than pH 9 during the electrophoresis) is beyond the optimum pH (~7) for the phosphate trapping of  $Zn^{2+}$ -Phos-tag (4). Therefore, we investigated the other metal complex acting as a phosphate-trapping molecule at an alkaline pH. The phosphate binding of the Phos-tag metal complex at pH 9 was confirmed by MALDI-TOF-MS using phenyl phosphate, phosphoserine, and phosphotyrosine as typical phosphates ( $ROPO_3^-$ ) in the presence of 2

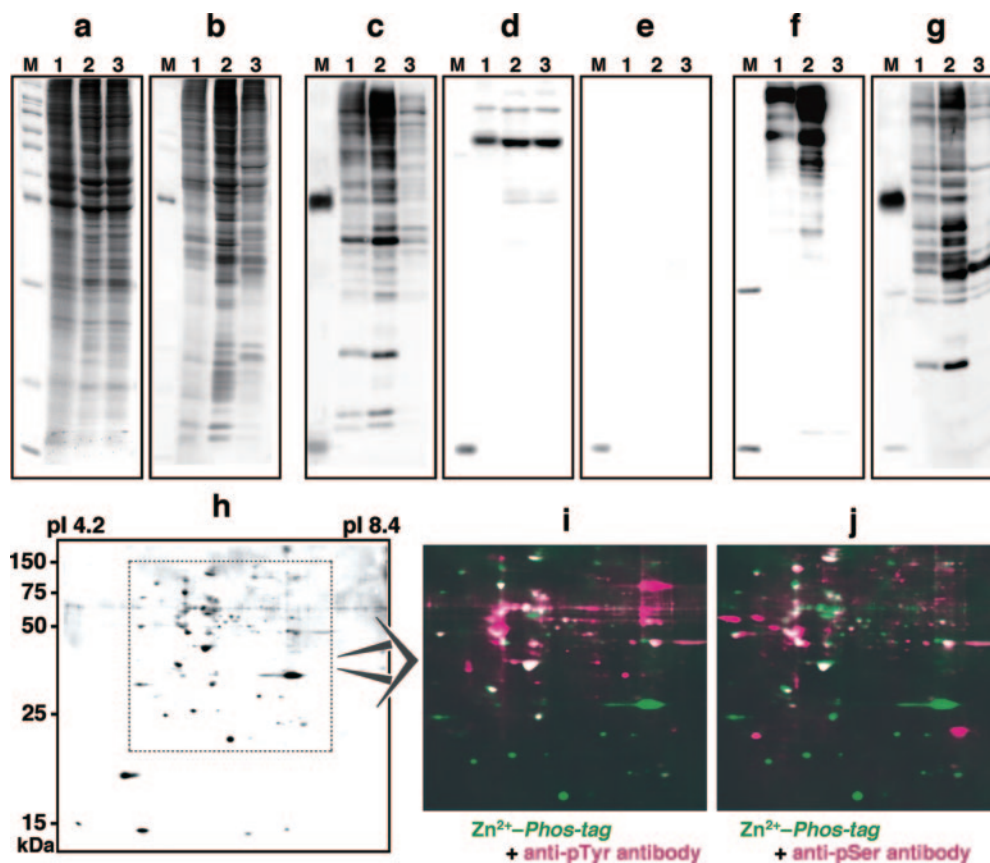


**FIG. 3. Comparison of different detection methods for one-dimensional SDS-PAGE (a–g) and 2-D IEF/SDS-PAGE (h–j) of A431 cell lysate.** a, fluorescent gel staining with SYPRO Ruby (*i.e.* staining of all proteins). b, fluorescent gel staining with Pro-Q Diamond (*i.e.* staining of the phosphorylated protein). c, electroblotting analysis (chemiluminescence detection) using biotin-pendant  $Zn^{2+}$ -Phos-tag and HRP-SA. d, electroblotting analysis (chemiluminescence detection) using HRP-SA. e, electroblotting analysis (chemiluminescence detection) using the HRP-SA complex with the biotin-pendant Phos-tag ligand in the presence of 1 mM EDTA. f, electroblotting analysis (chemiluminescence detection) using the HRP-anti-Tyr(P) antibody. g, electroblotting analysis (chemiluminescence detection) using the anti-Ser(P) antibody and the HRP-anti-IgG antibody. Each lane (a–g) contains 7.5  $\mu$ g of protein of the A431 cell lysate before (lane 1) or after (lane 2) EGF stimulation or 7.5  $\mu$ g of protein of the AP-treated lysate of EGF-stimulated A431 cells (lane 3). The molecular mass standards (205, 116, 97, 80, 66, 55, 45 (ovalbumin), 30, 21, and 14 (lysozyme) kDa from the top) are shown in lane M. h, electroblotting 2-D analysis (chemiluminescence detection) of the EGF-stimulated A431 cell lysate (50  $\mu$ g of proteins) using biotin-pendant  $Zn^{2+}$ -Phos-tag and HRP-SA. The blot was successively probed with the HRP-anti-Tyr(P) antibody and the anti-Ser(P) antibody/HRP-anti-IgG antibody. Shown are superimposed images of the area surrounded with a dotted square in h: i, using biotin-pendant  $Zn^{2+}$ -Phos-tag (green) and the anti-Tyr(P) antibody (magenta); j, using biotin-pendant  $Zn^{2+}$ -Phos-tag (green) and the anti-Ser(P) antibody (magenta). Proteins detected by both methods appear as white spots in i and j. pSer, phosphoserine; pTyr, phosphotyrosine.

eq. of metal(II) ions (*i.e.*  $Mn^{2+}$ ,  $Cu^{2+}$ ,  $Co^{2+}$ ,  $Fe^{2+}$ , and  $Ni^{2+}$ ). The acrylamide-pendant Phos-tag ligand showed remarkable MS signals of the 1:1 phosphate-binding manganese(II) complexes (*i.e.*  $ROPO_3^{2-}$ -[acrylamide-pendant  $Mn^{2+}$ -Phos-tag] $^{3+}$ , see Supplemental Fig. 3). Similar MALDI-TOF-MS signals for corresponding 1:1 phosphate complexes with  $Zn^{2+}$ -Phos-tag have been reported at a neutral pH (5).

On the basis of the MALDI-TOF-MS results, we conducted SDS-PAGE using polyacrylamide-bound  $Mn^{2+}$ -Phos-tag. Fig. 4 shows the effect of  $Mn^{2+}$ -Phos-tag on the mobility of phosphorylated proteins ( $\alpha$ -casein,  $\beta$ -casein, and ovalbumin) in SDS-PAGE by subsequent CBB staining. In the absence of polyacrylamide-bound  $Mn^{2+}$ -Phos-tag (*i.e.* normal SDS-PAGE), the mobilities of  $\alpha$ -casein and dephosphorylated

$\alpha$ -casein (Fig. 4a, lane at 0  $\mu$ M), of  $\beta$ -casein and dephosphorylated  $\beta$ -casein (Fig. 4b, lane at 0  $\mu$ M), and of ovalbumin and dephosphorylated ovalbumin (Fig. 4c, lane at 0  $\mu$ M) are almost the same. In the presence of polyacrylamide-bound  $Mn^{2+}$ -Phos-tag (50, 100, and 150  $\mu$ M), a difference in mobility between the phosphorylated proteins and the corresponding dephosphorylated proteins (*i.e.* a mobility shift of the phosphorylated protein against the dephosphorylated protein) is observed. The polyacrylamide-bound Phos-tag ligand without  $Mn^{2+}$  ions did not show any mobility shifts of phosphorylated proteins (data not shown). The  $R_f$  values of all samples become smaller dose-dependently in comparison with those in the absence of  $Mn^{2+}$ -Phos-tag; this is possibly due to electrostatic interaction between cationic  $Mn^{2+}$ -Phos-tag and an-

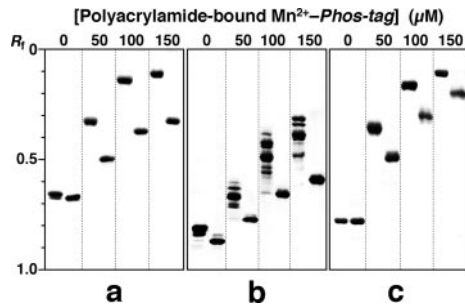


FIG. 4. SDS-PAGE of phosphorylated proteins and the corresponding dephosphorylated proteins in the absence and presence of polyacrylamide-bound  $\text{Mn}^{2+}$ -Phos-tag (50, 100, and 150  $\mu\text{M}$ ). a,  $\alpha$ -casein with 10% polyacrylamide gel. b,  $\beta$ -casein with 10% polyacrylamide gel. c, ovalbumin with 7.5% polyacrylamide gel. The phosphorylated and dephosphorylated proteins (0.30  $\mu\text{g}$  of protein/lane) were applied in the left and right lanes, respectively, for each run of electrophoresis. The  $R_f$  value of 1.0 is defined as the position of bromphenol blue dye. All SDS-PAGE gels were stained with CBB dye.

ionic SDS-bound proteins. Interestingly  $\beta$ -casein appears as eight bands using 100  $\mu\text{M}$   $\text{Mn}^{2+}$ -Phos-tag (see Fig. 4b), indicating the existence of at least eight isotypes with a different number of phosphomonoester dianions.

**Simultaneous Determination on Phosphorylated and Dephosphorylated Proteins**—We quantitatively monitored the enzymatic incorporation or removal of phosphate into proteins using  $\text{Mn}^{2+}$ -Phos-tag SDS-PAGE and CBB staining (see Fig. 5). Normal SDS-PAGE analyses showed that the total protein (the amount of a substrate for kinase or phosphatase) applied at each incubation time was almost equal. In the kinase assays of Abl (Fig. 5a, Abltide-GST as a substrate) and MAP kinase (Fig. 5b, MBP as a substrate) followed by 100  $\mu\text{M}$   $\text{Mn}^{2+}$ -Phos-tag SDS-PAGE and CBB staining, the slower (higher) migration bands increased time-dependently, whereas the faster (lower) migration bands decreased. Successive immunoblotting analyses using the anti-Tyr(P) antibody (Fig. 5a) and the anti-pMBP antibody (which recognizes the phosphorylated Thr<sup>97</sup> residue) (Fig. 5b) showed that the slower migration bands are phosphorylated proteins. Treatment of the  $\text{Mn}^{2+}$ -Phos-tag SDS-PAGE gel with EDTA before the immunoblotting analyses is necessary for efficient transfer of the phosphorylated proteins to a PVDF membrane without trapping by the Phos-tag molecule (see “Experimental Procedures”). In the phosphatase assays of AP (Fig. 5c,  $\beta$ -casein as a substrate) and TC-PTP (Fig. 5d, phosphorylated Abltide-GST as a substrate) followed by  $\text{Mn}^{2+}$ -Phos-tag SDS-PAGE and CBB staining, the slower (higher) migration bands decreased time-dependently, whereas the faster (lower) migration bands increased. These results indicate that acrylamide-pendant  $\text{Mn}^{2+}$ -Phos-tag preferentially captures phosphomonoester dianions bound to Ser, Thr, and Tyr residues as well as biotin-pendant  $\text{Zn}^{2+}$ -Phos-tag. Thus,  $\text{Mn}^{2+}$ -Phos-tag SDS-PAGE has enabled the simultaneous determination of phosphorylated and corresponding dephosphorylated proteins in a polyacrylamide gel.

## DISCUSSION

In this report, we have described two methods using Phos-tag molecules for the visualization of protein phosphorylation and dephosphorylation. The methods are independent on the amino acid residues; thus, protein phosphorylation can be comprehensively detected. One method is the application of biotin-pendant  $\text{Zn}^{2+}$ -Phos-tag and HRP-SA to Western blotting analysis: protein samples are first separated by electrophoresis and then electroblotted to a PVDF membrane and detected as ECL signals. We succeeded in the sensitive and specific detection of phosphorylated proteins on serine, threonine, and tyrosine residues using the ECL system. The blot-staining method has a general advantage over gel-staining methods with regard to the long term storage of protein-blotted membranes. The other method is the application of polyacrylamide-bound  $\text{Mn}^{2+}$ -Phos-tag to SDS-PAGE for the separation of phosphorylated proteins in the gel. By means of the subsequent general method of CBB staining, phosphorylated proteins can be visualized as a slower migration band compared with a corresponding dephosphorylated protein. This quantitative method revealed the existence of the isotypes of a multiphosphorylated protein (e.g.  $\beta$ -casein) as different migration bands. Additionally it is appropriate for the screening of an activator or an inhibitor of protein kinase and phosphatase.

The biotin-pendant  $\text{Zn}^{2+}$ -Phos-tag was reported as a novel probe of multiphosphopeptides to detect the on-chip phosphorylations by the SPR imaging technique (9). Previously another SPR detection system with the anti-Tyr(P) antibody was proposed (24). Antibodies whose epitopes are Ser(P), Thr(P), or Tyr(P) are commercially available and can be applied to phosphorylation detection on the SPR. However, multiple antibodies are required for the peptide array on which many kinase substrates are immobilized. Therefore, the Phos-tag molecule, which is not dependent on the amino acid residue, was very useful in a system with an array format. In a similar fashion, it is worthwhile to consider using the biotin-pendant  $\text{Zn}^{2+}$ -Phos-tag in Western blotting analysis for evaluating whole phosphorylated proteins from the cell lysate on a PVDF membrane. In addition, the application can increase the chances of finding a new phosphorylated protein. Classical detection of phosphorylated proteins usually requires the use of autoradiography after the incorporation of isotopic [<sup>32</sup>P]orthophosphate into cultured cells or subcellular fractions by protein kinases (14–21). However, this approach is limited to specimens amenable to radiolabeling and poses certain safety and disposal problems. Furthermore phosphorylated proteins on a PVDF membrane can be detected by immunoblotting analysis using antibodies against phosphorylated amino acid residues (25–27). Unfortunately the specificity of antibodies depends on the quality of the antibody, and the antibodies are often sensitive to the amino acid sequence context. Although a few high quality clones of anti-

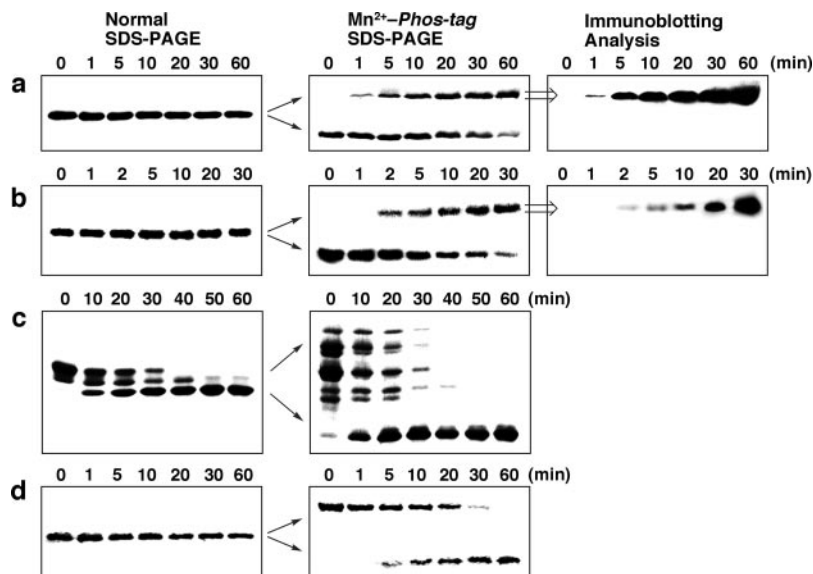


FIG. 5. Kinase and phosphatase assays by  $\text{Mn}^{2+}$ -Phos-tag SDS-PAGE (10–12.5% polyacrylamide containing 100  $\mu\text{M}$  polyacrylamide-bound  $\text{Mn}^{2+}$ -Phos-tag). *a*, phosphorylation of Abl-GST (0.10  $\mu\text{g}$  of protein/lane) incubated with Abl in 12.5% polyacrylamide gel. After  $\text{Mn}^{2+}$ -Phos-tag SDS-PAGE, immunoblotting analysis (chemiluminescence detection) was conducted using the HRP-anti-Tyr(P) antibody. *b*, phosphorylation of MBP (0.56  $\mu\text{g}$  of protein/lane) incubated with MAP kinase in 12.5% polyacrylamide gel. After  $\text{Mn}^{2+}$ -Phos-tag SDS-PAGE, immunoblotting analysis (chemiluminescence detection) was conducted using the anti-pMBP antibody/HRP-anti-IgG antibody. *c*, dephosphorylation of  $\beta$ -casein (0.30  $\mu\text{g}$  of protein/lane) incubated with AP in 10% polyacrylamide gel. *d*, dephosphorylation of phosphorylated Abl-GST (0.10  $\mu\text{g}$  of protein/lane) incubated with a tyrosine phosphatase, TC-PTP, in 12.5% polyacrylamide gel. The incubation time is shown above each lane. Normal SDS-PAGE and  $\text{Mn}^{2+}$ -Phos-tag SDS-PAGE gels were stained with CBB dye.

bodies to phosphorylated tyrosine are commercially available, the binding specificities of some anti-Ser(P) and anti-Thr(P) antibodies are dependent on the microenvironmental structures of phosphorylated residues in the proteins. Compared with these traditional approaches, our established method offers significant advantages. (i) The radioactivity is avoided. (ii) The blocking treatment of a PVDF membrane is not necessary. (iii) The binding specificity of the Phos-tag molecule is independent of the amino acid sequence context. Furthermore the Phos-tag method can be fully followed by downstream procedures, such as antibody reprobing, mass spectrometry, or Edman sequencing.

The  $\text{Mn}^{2+}$ -Phos-tag was utilized as a novel phosphate affinity SDS-PAGE. The polyacrylamide-bound  $\text{Mn}^{2+}$ -Phos-tag showed preferential trapping of the phosphorylated proteins without disordering (waving or tailing of protein bands) of the migration image. The 1:1 phosphate-bound  $\text{Mn}^{2+}$ -Phos-tag complexes were confirmed by MALDI-TOF-MS at an alkaline pH for the general SDS-PAGE. A relevant x-ray crystal structure of the dimanganese complex with the Phos-tag ligand (alkoxide form) was reported as an acetate-bridging species (28). Our established method requires a general minislab PAGE system and an additive, acrylamide-pendant  $\text{Mn}^{2+}$ -Phos-tag without any special apparatuses, radioisotopes, or fluorescent probes. The  $\text{Mn}^{2+}$ -Phos-tag SDS-PAGE can identify the time course ratio of phosphorylated and dephosphorylated proteins in an SDS-PAGE gel.

The phosphorylation status of a particular protein is deter-

mined by the equilibrium of the opposing activities of protein kinase and phosphatase. Perturbations in the equilibrium fundamentally affect the numbers of cellular events and are also involved in many diseases. Therefore, the development of a more specific and efficient method to detect protein phosphorylation has attracted great interest toward phosphoproteome studies in the biological and medical fields. We believe that phosphoproteomics would progress greatly by combining our Phos-tag technology and existing methods using high quality antibodies (27) and convenient mass spectrometers (3, 29, 30).

\* This work was supported by Grants-in-aid for Scientific Research (B) 15390013 and for Young Scientists (B) 17790034 from the Ministry of Education, Culture, Sports, Science, and Technology of Japan and by a research grant from Hiroshima University Fujii Foundation. The costs of publication of this article were defrayed in part by the payment of page charges. This article must therefore be hereby marked "advertisement" in accordance with 18 U.S.C. Section 1734 solely to indicate this fact.

§ The on-line version of this article (available at <http://www.mcponline.org>) contains supplemental material.

¶ To whom correspondence may be addressed. Tel.: 81-82-257-5281; Fax: 81-82-257-5336; E-mail: kinoeiji@hiroshima-u.ac.jp.

|| To whom correspondence may be addressed. Tel.: 81-82-257-5281; Fax: 81-82-257-5336; E-mail: tkoike@hiroshima-u.ac.jp.

#### REFERENCES

- Hunter, T. (1995) Protein kinases and phosphatases: the yin and yang of protein phosphorylation and signaling. *Cell* **80**, 225–236
- Hunter, T. (2000) Signaling—2000 and beyond. *Cell* **100**, 113–127



3. Ohtsu, I., Nakanishi, T., Furuta, M., Ando, E., and Nishimura, O. (2005) Direct matrix-assisted laser desorption/ionization time-of-flight mass spectrometric identification of proteins on membrane detected by western blotting and lectin blotting. *J. Proteome Res.* **4**, 1391–1396
4. Kinoshita, E., Takahashi, M., Takeda, H., Shiro, M., and Koike T. (2004) Recognition of phosphate monoester dianion by an alkoxide-bridged dinuclear zinc(II) complex. *Dalton Trans.* 1189–1193
5. Takeda, H., Kawasaki, A., Takahashi, M., Yamada, A., and Koike, T. (2003) Matrix-assisted laser desorption/ionization time-of-flight mass spectrometry of phosphorylated compounds using a novel phosphate capture molecule. *Rapid Commun. Mass Spectrom.* **17**, 2075–2081
6. Hirano, K., Matsui, H., Tanaka, T., Matsuura, F., Satouchi, K., and Koike, T. (2004) Production of 1,2-didocosahexaenoyl phosphatidylcholine by bonito muscle lysophosphatidylcholine/transacylase. *J. Biochem. (Tokyo)* **136**, 477–483
7. Tanaka, T., Tsutsui, H., Hirano, K., Koike, T., Tokumura, A., and Satouchi, K. (2004) Quantitative analysis of lysophosphatidic acid by time-of-flight mass spectrometry using a phosphate-capture molecule. *J. Lipid Res.* **45**, 2145–2150
8. Kinoshita, E., Yamada, A., Takeda, H., Kinoshita-Kikuta, E., and Koike, T. (2005) Novel immobilized zinc(II) affinity chromatography for phosphopeptides and phosphorylated proteins. *J. Sep. Sci.* **28**, 155–162
9. Inamori, K., Kyo, M., Nishiya, Y., Inoue, Y., Sonoda, T., Kinoshita, E., Koike, T., and Katayama, Y. (2005) Detection and quantification of on-chip phosphorylated peptides by surface plasmon resonance imaging techniques using a phosphate capture molecule. *Anal. Chem.* **77**, 3979–3985
10. Steinberg, T. H., Agnew, B. J., Gee, K. R., Leung, W. Y., Goodman, T., Schulenberg, B., Hendrickson, J., Beechem, J. M., Haugland, R. P., and Patton, W. F. (2003) Global quantitative phosphoprotein analysis using multiplexed proteomics technology. *Proteomics* **3**, 1128–1144
11. Berggren, K., Chernokalskaya, E., Steinberg, T. H., Kemper, C., Lopez, M. F., Diwu, Z., Haugland, R. P., and Patton, W. F. (2000) Background-free, high sensitivity staining of proteins in one- and two-dimensional sodium dodecyl sulfate-polyacrylamide gels using a luminescent ruthenium complex. *Electrophoresis* **21**, 2509–2521
12. Laemmli, U. K. (1970) Cleavage of structural proteins during the assembly of the head of bacteriophage T4. *Nature* **227**, 680–685
13. Carpenter, G., and Cohen, S. (1979) Epidermal growth factor. *Annu. Rev. Biochem.* **48**, 193–216
14. Carpenter, G., King, L., Jr., and Cohen, S. (1979) Rapid enhancement of protein phosphorylation in A-431 cell membrane preparations by epidermal growth factor. *J. Biol. Chem.* **254**, 4884–4891
15. Cohen, S., Carpenter, G., and King, L., Jr. (1980) Epidermal growth factor-receptor-protein kinase interactions. Co-purification of receptor and epidermal growth factor-enhanced phosphorylation activity. *J. Biol. Chem.* **255**, 4834–4842
16. Linsley, P. S., and Fox, C. F. (1980) Controlled proteolysis of EGF receptors: evidence for transmembrane distribution of the EGF binding and phosphate acceptor sites. *J. Supramol. Struct.* **14**, 461–471
17. Hunter, T., and Cooper, J. A. (1981) Epidermal growth factor induces rapid tyrosine phosphorylation of proteins in A431 human tumor cells. *Cell* **24**, 741–752
18. Cooper, J. A., and Hunter, T. (1981) Similarities and differences between the effects of epidermal growth factor and Rous sarcoma virus. *J. Cell Biol.* **91**, 878–883
19. Ghosh-Dastidar, P., and Fox, C. F. (1983) Epidermal growth factor and epidermal growth factor receptor-dependent phosphorylation of a  $M_r = 34,000$  protein substrate for pp60<sup>src</sup>. *J. Biol. Chem.* **258**, 2041–2044
20. Meisenhelder, J., Suh, P. G., Rhee, S. G., and Hunter, T. (1989) Phospholipase C- $\gamma$  is a substrate for the PDGF and EGF receptor protein-tyrosine kinases in vivo and in vitro. *Cell* **57**, 1109–1122
21. Li, S., Couvillon, A. D., Brasher, B. B., and Van Etten, R. A. (2001) Tyrosine phosphorylation of Grb2 by Bcr/Abl and epidermal growth factor receptor: a novel regulatory mechanism for tyrosine kinase signaling. *EMBO J.* **20**, 6793–6804
22. Lim, Y. P., Diong, L. S., Qi, R., Druker, B. J., and Epstein, R. J. (2003) Phosphoproteomic fingerprinting of epidermal growth factor signaling and anticancer drug action in human tumor cells. *Mol. Cancer Ther.* **2**, 1369–1377
23. Chelius, D., Zhang, T., Wang, G., and Shen, R. F. (2003) Global protein identification and quantification technology using two-dimensional liquid chromatography nanospray mass spectrometry. *Anal. Chem.* **75**, 6658–6665
24. Houseman, B. T., Huh, J. H., Kron, S. J., and Mrksich, M. (2002) Peptide chips for the quantitative evaluation of protein kinase activity. *Nat. Biotechnol.* **20**, 270–274
25. Czernik A. J., Girault, J. A., Nairn, A. C., Chen, J., Snyder, G., Kebejian, J., and Greengard, P. (1991) Production of phosphorylation state-specific antibodies. *Methods Enzymol.* **201**, 264–283
26. Epstein, R. J., Druker, B. J., Roberts, T. M., and Stiles, C. D. (1992) Synthetic phosphopeptide immunogens yield activation-specific antibodies to the c-erbB-2 receptor. *Proc. Natl. Acad. Sci. U. S. A.* **89**, 10435–10439
27. Kaufmann, H., Bailey, J. E., and Fussenegger, M. (2001) Use of antibodies for detection of phosphorylated proteins separated by two-dimensional gel electrophoresis. *Proteomics* **1**, 194–199
28. Suzuki, M., Sugisawa, T., Senda, H., Oshio, H., and Uehara, A. (1989) Synthesis and characterization of a novel tetranuclear manganese(II-III,III,II) mixed valence complex. *Chem. Lett.* 1091–1094
29. Sloane, A. J., Duff, J. L., Wilson, N. L., Gandhi, P. S. Hill, C. J., Hopwood, F. G. Smith, P. E., Thomas, M. L., Cole, R. A., Packer, N. H., Breen, E. J., Cooley, P. W., Wallace, D. B., Williams, K. L., and Gooley, A. A. (2002) High throughput peptide mass fingerprinting and protein microarray analysis using chemical printing strategies. *Mol. Cell. Proteomics* **1**, 490–499
30. Nakanishi, T., Ohtsu, I., Furuta, M., Ando, E., and Nishimura, O. (2005) Direct MS/MS analysis of proteins blotted on membranes by a matrix-assisted laser desorption/ionization-quadrupole ion trap-time-of-flight tandem mass spectrometer. *J. Proteome Res.* **4**, 743–747